Low Length Dispersity Fiber-Like Micelles from an A-B-A Triblock Copolymer with Terminal Crystallizable Poly(ferrocenyldimethylsilane) Segments via Living Crystallization-Driven Self-Assembly

Qiwei Zhang[1, 2], *Yunxiang He*[2], *Alex M. Oliver*[2], *Samuel Pearce*[2], *Robert L. Harniman*[2], *George R. Whittell*[2], *Yanju Liu*[3], *Shanyi Du*[1], *Jinsong Leng**[, 1] *and Ian Manners**[, 2, 4]

[1]National Key Laboratory of Science and Technology on Advanced Composites in Special Environments, Harbin Institute of Technology, Harbin Institute of Technology, Harbin 150080, China

[2]School of Chemistry, University of Bristol, Bristol BS8 1TS, United Kingdom

[3]Department of Astronautical Science and Mechanics, Harbin Institute of Technology, Harbin 150080, China

[4]Department of Chemistry, University of Victoria, Victoria, BC V8W 3V6, Canada

[*]To whom correspondence should be addressed: lengjs@hit.edu.cn and imanners@uvic.ca

Abstract

Solution self-assembly of a linear ABA triblock copolymer with two terminal crystallizable poly(ferrocenyldimethylsilane) (PFS) core-forming "A" blocks and a central poly(dimethylsiloxane) (PDMS) corona-forming "B" block has been investigated. The low dispersity (D = 1.05) copolymer, PFS_{26}-*b*-$PDMS_{584}$-*b*-PFS_{26} (block ratio 1.0 : 22.5 : 1.0) , was prepared through a combination of living anionic polymerization and end-to-end coupling. The block ratio and dispersity were established by a combination of MALDI-TOF mass spectrometry, ^{1}H NMR, and GPC. Individual 1D fiber-like micelles with looped PDMS coronas were formed in mixed solvents of hexane and decane. Low length-dispersity fiber-like micelles of controlled length were prepared from short seed micelles of PFS_{26}-*b*-$PDMS_{584}$-*b*-PFS_{26} derived from sonication using the seeded growth method termed living crystallization-driven self-assembly. In addition, seeded growth of blends of both PFS_{26}-*b*-$PDMS_{584}$-*b*-PFS_{26} and PFS_{26} homopolymer and of PFS_{26}-*b*-$PDMS_{584}$-*b*-PFS_{26} and the analogous diblock copolymer PFS_{26}-*b*-$PDMS_{292}$ were also explored. Large aggregates with fiber-like protrusions were formed by spontaneous nucleation of the blends of PFS_{26}-*b*-$PDMS_{584}$-*b*-PFS_{26} and PFS_{26}. High-aspect ratio ribbon-like micelles were formed by adding the blends of PFS_{26}-*b*-$PDMS_{584}$-*b*-PFS_{26} and PFS_{26} to the cylindrical PFS_{26}-*b*-$PDMS_{584}$-*b*-PFS_{26} seeds. In contrast, surprisingly, seeded growth of blends of PFS_{26}-*b*-$PDMS_{584}$-*b*-PFS_{26} and PFS_{26}-*b*-$PDMS_{292}$ or the individual components using seeds of either PFS_{26}-*b*-$PDMS_{584}$-*b*-PFS_{26} or PFS_{26}-*b*-$PDMS_{292}$ showed that growth is only detected in the case of matching of the seed and multiblock copolymer chemistries.

Introduction

Self-assembly of block copolymers (BCPs) has attracted growing and extensive attention as a powerful approach to functional self-assembled nanostructures over the past two decades. [1-4] Well-defined BCP architectures have been realized using synthetic methods including living anionic polymerization and controlled radical polymerization.[2, 3] BCP self-assembly allows access to a broad variety morphologies either in bulk or thin-films, or in the solution state in solvents that are selective for one of the blocks.[4] Core-corona nanoparticles (micelles) formed in selective solvents have found applications in the areas such as drug delivery,[5, 6] catalysis,[7] electronics and photoelectric devices,[8, 9].

In recent years, the solution self-assembly a variety of amphiphilic BCPs, including AB diblock copolymers, ABC linear triblock terpolymers, and multi-arm star polymers, has been used to prepare complex nanostructures with either core or corona compartmentalization.[10] ABA triblock copolymers consisting of one solvophilic central block and two solvophobic terminal segments have rarely been studied in terms of their self-assembly behaviour. Most previous studies focused on intermicellar association by which the terminal A segments participate in core formation in different micelles to create physically crosslinked transient networks at high concentration.[11, 12] However, at low concentration in a selective solvent for the central B block, individual "flowerlike" micelles are accessible whereby the two terminal A segments contribute to the core in the same micelle. These micelles can possess interesting properties such as a lower critical micelle concentration (CMC), and higher kinetic stability relative to their "starlike" counterparts formed by deblock copolymer analogues.[13, 14] Until now, only a few triBCPs have been found to self-assemble into flowerlike micelles. In these cases the looped solvated central A blocks comprise polymers such as poly(ethyleneglycol) (PEG)[15-20] and poly(N-isopropylacrylamide) (PNIPAM)[21-23]. The majority of these investigations tend to focus on spherical micelles and their transitions induced by temperature, concentration, composition or pH. The preparation of individual flowerlike micelles with less common morphologies such as fibers is virtually unexplored.

A process known as "crystallization-driven self-assembly" (CDSA) in selective solvents has recently provided routine access to pure samples of more challenging to acquire morphologies

such as fibers or platelets.[4, 24, 25] Furthermore, the preparation of samples with controlled and uniform dimensions has been achieved for these 1D or 2D micelles by the use of "living CDSA", a seeded-growth process that functions in an analogous manner to living covalent polymerizations.[26, 27] The use of poly(ferrocenyldimethylsilane) (PFS)[28] as a crystallizable core-forming block for living CDSA has been extensively studied and the approach has recently been extended to many other crystallizable materials[29-34]. The living CDSA of AB diblock copolymers with one crystallizable segment to generate 1D and 2D assemblies has been well studied in previous work.[27, 33, 35] Moreover, linear and star ABC triblock copolymers which form the micelles with "patchy" coronas has also been presented.[36] However, no examples of living CDSA have been reported for BCPs with two crystallizable segments. In previous work, we studied poly(ferrocenyldimethylsilane)-*block*-poly(dimethylsiloxane)-*block*-poly(ferrocenyldimethylsilane) (PFS-*b*-PDMS-*b*-PFS) triblock copolymers by a transition-metal-catalyzed ROP methodology.[37] However, multiple micellar morphologies were found to coexist, possibly as a result if their substantial dispersity which results from the non-living nature of the synthetic procedure.[38] Furthermore, seeded growth of these triblock copolymer materials was not explored.

Herein, we report studies of the living CDSA of a well-defined, low dispersity PFS-*b*-PDMS-*b*-PFS triblock copolymer prepared via sequential living anionic polymerization of a ferrocenophane and hexamethylcyclotrisiloxane.[39, 40] We also present studies of the seeded growth of blends of PFS-*b*-PDMS-*b*-PFS triblock copolymer with PFS homopolymer and the corresponding PFS-*b*-PDMS diblock copolymer.

Experimental Section

Materials

Ferrocenophanes were prepared through the method reported in previous work.[39] *n*-Butyllithium (*n*-BuLi) (1.6 M in hexanes), dimethyldichlorosilane and hexamethylcyclotrisiloxane were purchased from Aldrich. Me_2SiCl_2 was dried over CaH_2 for 12 h before distillation. $[Me_2SiO]_3$ was sublimed at room temperature under a static vacuum prior to use. Tetrahydrofuran (THF) was distilled from Na/benzophenone under prepurified N_2 immediately before use. All the self-assembly experiments were performed in HPLC grade solvents that were acquired from Fisher.

Synthesis of PFS_{26}-*b*-$PDMS_{584}$-*b*-PFS_{26} triblock copolymer

Dimethylsila[1]ferrocenophane (100 mg, 0.413 mmol) was dissolved in dry THF (1 mL) in a glovebox (Mbraun, inert purified nitrogen atmosphere) at room temperature. n-butyllithium (1.6 M in hexane, 10.3 μL, 1.65×10^{-2} mmol) was added to the rapidly stirring solution in one portion. After 30 mins, the colour of the reaction mixture could change from red to amber. An aliquot was then taken from the reaction mixture before the rapid addition of $[Me_2SiO]_3$ (305 mg, 1.37 mmol). After another 1 h, aliquot was taken again and the remaining reaction mixture was transferred from the glove box to a Schlenk tube attached to a standard Schlenk line under a nitrogen atmosphere. A solution of 9 μL of 0.9 M Me_2SiCl_2 (8.1×10^{-3} mmol) in THF was then added while stirring. The mixture was precipitated in methanol and centrifuged three times before drying in a vacuum oven overnight. Thus, yielded 154 mg (38%) of the yellow powdery ABA triblock copolymer was isolated by silica gel column chromatography in THF. The homopolymer and diblock copolymer could also be obtained terminating the reaction sequence at the appropriate earlier stage. Further characterisation outlined in the Supporting Information (SI).

Self-assembly of PFS_{26}-*b*-$PDMS_{584}$-*b*-PFS_{26} Triblock copolymers

A 100 μL aliquot of a PFS_{26}-*b*-$PDMS_{584}$-*b*-PFS_{26} unimer solution (10 mg/mL in THF) was added to three separate 5 mL vials. After the solvent was dried over by a nitrogen flow, 5 mL of *n*-hexane, *n*-decane, and *n*-hexane/ *n*-decane (1:1, *v*/*v*) were added to the vials separately. The solution obtained (0.2 mg/mL) was heated to 60 °C for 1 h and subsequently cooled to room temperature to prepare polydisperse cylindrical micelles by self-nucleation.

Living CDSA of PFS_{26}-*b*-$PDMS_{584}$-*b*-PFS_{26} Triblock Copolymer

The solution of cylindrical micelles was placed in an ice-water bath and sonicated by a sonotrode (Hielscher MS1, installed on Hielscher UP50H, 30 kHz/50 W) for 1 h. 50 μL colloidal solution of small PFS_{26}-*b*-$PDMS_{584}$-*b*-PFS_{26} micelle seeds (0.2 mg/mL, in *n*-hexane/ *n*-decane mixed solvent) was added to 0.4 mL mixed solvent of n-hexane and *n*-decane. After manually shaking for 10 s, 5, 10 and 20 μL PFS_{26}-*b*-$PDMS_{584}$-*b*-PFS_{26} unimers in THF (10 mg/mL) were injected into the solution, respectively. Another 10 s shaking was then performed and the achieved solution was left to age overnight at room temperature.

Self-assembly Experiments

A solution of a PFS_{26}-*b*-$PDMS_{584}$-*b*-PFS_{26} / PFS_{26} blend as unimers was prepared with a mass ratio of 1:1 as 10 mg/mL (overall concentration) in THF first. 100 μL solution was transferred to a 5 mL vial and THF was removed by a nitrogen flow. 5 mL of mixed solvent (*n*-hexane/ *n*-decane, 1:1, *v*:*v*) was added to the vial followed by heating the solution at 60 ºC for 1 h. The solution was cooled down and aged for 12 h to realize micelle formation through self-nucleation.

A 50 μL portion of a colloidal solution of small PFS_{26}-*b*-$PDMS_{584}$-*b*-PFS_{26} micelle seeds (0.2 mg/mL, in *n*-hexane/ *n*-decane mixed solvent) was added to three 5 mL vials with 0.4 mL mixed solvent of n-hexane and *n*-decane, respectively. 2.5 μL , 5 μL and 10 μL solution of PFS_{26}/PFS_{26}-*b*-$PDMS_{584}$-*b*-PFS_{26} blend unimer was then respectively added and the solution was allowed to be aged overnight at room temperature.

We also attempted seeded growth of a blend of PFS_{26}-*b*-$PDMS_{292}$/PFS_{26}-*b*-$PDMS_{584}$-*b*-PFS_{26} in the unimer state which were made up with a mass ratio of 1:1 as 10 mg/mL (overall concentration) in THF. The solutions of PFS_{26}-*b*-$PDMS_{292}$ seed micelles (0.2 mg/mL in *n*-hexane) and PFS_{26}-*b*-$PDMS_{584}$-*b*-PFS_{26} seed micelles (0.2 mg/mL in *n*-hexane/ *n*-decane mixed solvent) were diluted to 0.01 mg/mL. 10 μL and 20 μL solution of blend unimers was added to these solutions, respectively. The obtained solutions were then manually shaken for another 10 s and aged for 12 h at room temperature. The PFS_{26}-*b*-$PDMS_{292}$ unimer and PFS_{26}-*b*-$PDMS_{584}$-*b*-PFS_{26} unimer were respectively added to the solutions of seed micelles formed by PFS_{26}-*b*-$PDMS_{584}$-*b*-PFS_{26} and PFS_{26}-*b*-$PDMS_{292}$ as control experiments. Variations on these conditions such as the use of hexane/decane 1:1, pure hexane, pure decane, hexane/10% THF or

decane/10% THF by volume or the application of a mixture of PFS_{26}-*b*-$PDMS_{292}$ and PFS_{26}-*b*-$PDMS_{584}$-*b*-PFS_{26} seed micelles gave similar results to those described in Figure 7 and the accompanying discussion in the main text. Attempts to identify unconsumed unimer by UV-vis spectroscopy were thwarted by the low concentrations and aggregation and precipitation that were observed on increasing the concentration of the solution.

Characterization

Chemical structure and composition of PFS_{26}-b-$PDMS_{584}$-b-PFS_{26} triBCPs: The ^{1}H and ^{29}Si NMR spectra were obtained using a Varian 400 MHz spectrometer and all resonances were referenced to residual NMR solvent peaks. Molar masses were determined by gel permeation chromatography (GPC, Viscotek VE2001 GPCmax chromatograph) equipped with a triple detector array (UV/Vis detector, VE 3210, λ = 440 nm and dual angle laser light scattering detector, VE 270, 7° and 90°). THF (Fisher) was used as the eluent, with the flow rate set at 1 mL/min. Samples were dissolved in the eluent (1 mg/mL) and filtered through a Ministart SRP 15 filter (polytetrafluorethylene membrane, pore size = 0.45 μm) before analysis. The detectors were calibrated using polystyrene standards (Viscotek). Matrix-assisted laser desorption/ionization time-of-flight (MALDI-TOF) mass spectrometry was performed on a Bruker UltrafleXtreme 4700 instrument. The sample of PFS homopolymer was prepared in a solution of *trans*-2-[3-(4-*tert*-butylphenyl)-2-methyl-2-propenylidene]malononitrile matrix (20 mg/mL in THF) and the polymer (10 mg/mL in THF) in a 50 : 1 (v/v) ratio.

Morphological Analysis of PFS_{26}-b-$PDMS_{584}$-b-PFS_{26} micelles: Bright field transmission electron microscopy (TEM) micrographs were obtained on a JEOL JEM 1400 microscope operating at 120 kV and equipped with a Gatan Orius SC1000 CCD camera. Samples were prepared by drop-casting one drop (ca. 8 μL) of the micelle colloidal solution onto a carbon coated copper grid placed upon a piece of filter paper to remove excess solvent. Copper grids (400 mesh) were purchased from Agar Scientific and carbon films were prepared using a Quorum TEM Turbo Carbon Coater by sputtering carbon onto mica sheets. The carbon films were deposited onto the copper grids by floatation on water. The carbon coated grids were then allowed to dry for at least two days in air. Atomic force microscopy (AFM) height images were obtained using a Bruker Multimode 8 equipped with a ScanAsyst-HR fast scanning module and a ScanAsyst-Air-HR probe

with a tip radius of approximately 2 nm. The sample was prepared by drop-casting one drop (ca. 8 μL) of solution onto a carbon-coated TEM grid. Imaging was conducted in air at ambient temperature. Polydisperse micelle samples were sonicated using a Bandelin Sonorex Digitec DT 255 H sonic bath (ultrasonic nominal output = 160 W).

Results and Discussion

1. Synthesis and structural characterization of PFS_{26}-*b*-$PDMS_{584}$-*b*-PFS_{26} triblock copolymer

PFS_{26}-*b*-$PDMS_{584}$-*b*-PFS_{26} triblock copolymer was synthesized by a three-step protocol shown in Figure 1. First, the living anionic ROP of dimethylsila[1]ferrocenophane was used to form intermediates with living polymer ends.[39] After initiation by *n*-BuLi for 30 mins in THF at 25 °C, the living homopolymer was then reacted with $[Me_2SiO]_3$ for another 1 h. Finally, the triblock structure was formed by "coupling" two equivalents of living diblock copolymer with Me_2SiCl_2. The estimated molar mass after each step were tracked by GPC through aliquot removal. A significant increasing trend in molar mass (revealed by the shifts of the GPC peaks) could be observed in Figure 2. The estimated molar mass of final triblock copolymer ($M_n = 6.4\times10^4$ g/mol) was virtually double as the uncoupled diblock copolymer ($M_n = 3.3\times10^4$ g/mol), as expected for the coupling reaction between two living diblock copolymer chains. The remaining uncoupled PFS-*b*-PDMS diblock copolymer was removed by silica gel column chromatography (revealed by the disappearance of a low molecular weight shoulder). The molecular weight distribution of the obtained triblock copolymer (PDI = 1.05) is much narrower than that of the previously reported material formed by transition metal catalyzed ROP, a non-living method (PDI = 1.43)[37]. The composition of the synthesized triblock copolymer was determined by a combined analysis of the data from the MALDI-TOF mass spectrometry of the PFS homopolymer and ^{1}H NMR spectroscopic analysis of the triblock copolymer. The calculated degree of polymerization of PFS block was 26 according to the absolute molecular weight given by MALDI-TOF mass spectrometry and the repeat unit. The block ratio of the obtained triblock copolymer is approximately 1.0 : 22.5 : 1.0, as determined by ^{1}H NMR in Figure S1 through comparative integration of the cyclopentadienyl protons of PFS (δ = 4.00 ppm, 4.20 ppm) and the methyl protons of PDMS (δ = 0.05 ppm). Therefore, the final composition of the material could be corroborated as PFS_{26}-*b*-$PDMS_{584}$-*b*-PFS_{26} after comprehensive analysis of these data. The ^{29}Si

NMR spectrum (Figure S2) of this triBCP in CD_2Cl_2 shows intense resonances for the poly(ferrocenyldimethylsilane) segment (δ = -6.4 ppm) and the polysiloxane segments (δ = -21.3 ppm), respectively. No end groups or switching groups are observed due to the high molar mass and segmented nature of the material.

2. Self-Assembly of PFS_{26}-*b*-$PDMS_{584}$-*b*-PFS_{26} Triblock Copolymer

A small sample of triblock copolymer was used to produce the polydisperse cylindrical micelles through spontaneous nucleation (Figure 3a). We chose three selective solvents (*n*-hexane, *n*-decane and a 1:1 mixture of these solvents, respectively) for the PDMS corona-forming block to explore the influence of solvent selectivity on the solution self-assembly of PFS_{26}-*b*-$PDMS_{584}$-*b*-PFS_{26} triBCP. Each of these solutions with the concentration of 0.2 g/L was heated to 60 ^oC for 30 min, and then cooled to room temperature over 30 min. The samples obtained were aged for a minimum of 12 h before drop-casting onto a carbon-coated copper grid for TEM analysis after solvent evaporation. Figure 3b and 3c present the TEM data for the resulting fiber-like micelles of PFS_{26}-*b*-$PDMS_{584}$-*b*-PFS_{26} from the mixed solvent system (1:1 by volume) at different magnifications . Significantly, discrete polydisperse cylindrical micelles were exclusively formed in a 1:1 hexanes/decane solvent mixture. This indicates that the two terminal PFS core-forming blocks in the triblock copolymers do not become incorporated into separate micelles to form bridges to any significant degree which would lead to aggregates. Interestingly, the corresponding process in a pure hexanes or decane led to discrete cylindrical micelles coexisting with a thin film that presumably derived from unimers (Figure S4). The solubility parameter of mixed solvent appears more suitable for PFS_{26}-*b*-$PDMS_{584}$-*b*-PFS_{26} triBCP to generate fiber-like micelles compared with a single solvent. Again, no evidence for aggregates was detected. The absence of bridges between the micelles (Figure 3a, right) may be the result of the relatively low concentration of the solutions used for the self-nucleation experiments..

3. Seeded Growth/Living CDSA Studies Involving PFS_{26}-*b*-$PDMS_{584}$-*b*-PFS_{26} Triblock Copolymer

We also explored the living CDSA process for the PFS_{26}-*b*-$PDMS_{584}$-*b*-PFS_{26} triblock copolymer

(Figure 4a). Short seed micelles with a relatively narrow length distribution (L_n = 102 nm, L_w / L_n = 1.02, where L_w and L_n are the weight- and number-average length, respectively) were prepared by sonicating a solution of polydisperse cylinders (0.2 mg/mL in mixed solvent) for 1 h in an ice-water bath. Subsequently, selected amounts of PFS_{26}-*b*-$PDMS_{584}$-*b*-PFS_{26} unimer solution (10 mg/mL in THF) were added to the solutions of seed micelles corresponding to various unimer-to-seed ratios (5:1, 10:1 and 20:1). The resulting mixture was then stirred vigorously for 5 s and left to age for 24 h. TEM images of seed micelles and samples corresponding to each unimer-to-seed ratio after solvent evaporation are shown in Figure 4b to Figure 4e. The lengths of fiber-like micelles could be controlled with the increasing amount of PFS_{26}-*b*-$PDMS_{584}$-*b*-PFS_{26} unimers (L_n = 488 nm, 1058 nm and 1906 nm), and the length dispersity of the micelles was low in each case. In addition, there was no detectable alteration in the widths of the cores of the micelles (ca. 10 nm) observed in these images as a result of the high electron density of PFS which provides differential TEM contrast. The summary in Figure 4f and 4g demonstrates that the lengths of the micelles increase linearly with the unimer to seed ratio, which is one of the key characteristics of a living CDSA process.[41] Significantly, once again no physically crosslinked networks of micelles were formed in which the central PDMS segments bridge two different micelles. Based on these observations, it can be concluded that both PFS terminal blocks form the core of individual fiber-like micelles and that the PDMS coronal block loops to form flower-like structure (Figure 3a).

4. Comparative AFM Analysis of the Fiber-like Micelles formed by the Triblock Copolymer PFS_{26}-*b*-$PDMS_{584}$-*b*-PFS_{26} and the Diblock Copolymer PFS_{26}-*b*-$PDMS_{292}$

To provide comparative insight into the structures of fibers formed by the different block-type architectures, the fiber-like seed micelles of PFS_{26}-*b*-$PDMS_{584}$-*b*-PFS_{26} were analyzed by AFM. For comparison, we also prepared seeds micelles of PFS_{26}-*b*-$PDMS_{292}$ and subjected those to a similar analysis. AFM images showed that the average heights of these seed micelles were 6.1 nm and 7.7 nm, respectively (Figure 5). These values are only slightly smaller than the core widths (ca. 10 nm) of seed micelles observed by TEM. This suggests that the core cross-section is likely to be

close to circular (and possibly an oval shape) rather than rectangular. The observed height of PFS_{26}-*b*-$PDMS_{584}$-*b*-PFS_{26} seed fibers is slightly but consistently ca. 2 nm less than that for seeds of the corresponding diblock copolymer. This could be attributed to the looped structure of the PDMS chains in the fibers formed by the triblock copolymer which forces the coronal chains into a more constrained arrangement. This phenomenon could also be observed when comparing the width of PFS_{26}-*b*-$PDMS_{584}$-*b*-PFS_{26} seeds with that for PFS_{26}-*b*-$PDMS_{292}$ seeds. The core widths of these two types of seeds obtained by TEM are nearly the same (ca. 10 nm). However, from AFM images, the width of the core and corona of the triblock copolymer seeds (ca. 40 nm) is much smaller than that of the diblock copolymer (ca. 55 nm) (Figure 5). This difference is also attributed to the difference in coronal conformation.

5. Seeded Growth/Living CDSA of BCP Blends

To understand the influence of block-type architectures on the micelle morphology, we studied the self-assembly behaviour of a blend of PFS_{26}-*b*-$PDMS_{584}$-*b*-PFS_{26} with PFS_{26} homopolymer (1:1 mass ratio, mole ratio ~1:8). A solution of unimers (0.2 mg/mL) in a mixture of *n*-hexane and *n*-decane (*v* : *v*, 1 : 1) was heated to 60 °C, followed by subsequent cooling to room temperature. After aging for 12 h, a small aliquot of the solution was subject to TEM analysis after evaporating the solvent. As shown in Figure S5 large aggregates of predominantly fiber-like assemblies (> 5 μm in length) could be clearly observed. This phenomenon demonstrates the introduction of PFS homopolymer leads to a dramatic change in the morphology formed in self-assembly following self-nucleation. It is likely that PFS homopolymer crystallizes first as a result of its lower solubility in the solvent medium and that this subsequently induces epitaxial growth of the BCP to yield the observed fiber-like protrusions.

We also investigated the seeded growth of a mixture of PFS_{26}-*b*-$PDMS_{584}$-*b*-PFS_{26} and PFS_{26} unimers (Figure 6a) by adding a known amount of the unimer blend to a colloidal solution of seed micelles of PFS_{26}-*b*-$PDMS_{584}$-*b*-PFS_{26} triBCP (L_n = 102 nm, 0.2 mg/mL in mixed solvent). The total unimer to seed mass ratios were chosen as 2.5 : 1, 5 : 1 and 10 : 1, respectively. From TEM images in Figure 6b, 6c and 6d, we find that the use of blends could lead to high-aspect ratio ribbon-like micelles with increasing widths (ca. 20 nm, 25 nm and 35 nm, respectively). These

results present a different trend in comparison with the 1D micelles formed only by the triblock copolymers, which could be attributed to growth from the seeds in both terminal and lateral directions. Moreover, the generated micelles show a linear dependence of area instead of length on the unimer-to-seed ratio, which is consistent with a living CDSA process in 2D (Figure 6e).[27]

Next, we explored the seeded growth of blends of the triblock and diblock copolymers. A PFS_{26}-*b*-$PDMS_{292}$/PFS_{26}-*b*-$PDMS_{584}$-*b*-PFS_{26} blend (1:1 mass ratio, mole ratio 2:1) in the form of unimers (10 mg/mL in THF, overall concentration) was then separately introduced to the solutions of seed micelles of PFS_{26}-*b*-$PDMS_{292}$ and PFS_{26}-*b*-$PDMS_{584}$-*b*-PFS_{26} (112 nm and 102 nm, respectively) with two different unimer to seed ratios (mass ratio 10 : 1 and 20 : 1). The percentage of added unimers to pre-existing seeds in the two systems were 90.9 % and 95.2 %, respectively. Figure 7 shows TEM micrographs and histograms of the contour length distribution of the resulting cylindrical micelles. For the seed micelles of PFS_{26}-*b*-$PDMS_{584}$-*b*-PFS_{26}, the lengths of cylinders obtained by seeded growth were 477 nm and 922 nm for the 10 : 1 and 20 : 1 ratios, respectively. As previously discussed, the contour lengths of cylindrical micelles formed in a living CDSA process should show a linear dependence on the unimer-to-seed ratio. However, the length of the resulting cylinders was only half of the expected value with no detectable change in the micelle widths. Analogous results were obtained for the cylinders grown from the seed micelles of PFS_{26}-*b*-$PDMS_{292}$, which the contour lengths were measured as 509 nm (for the 10 : 1 unimer to seed ratio) and 931 nm (for the 20 : 1 ratio). These results, which were found to be consistent over a range of experimental variations, are indicative of the surprising explanation that the unimers only effectively grow from the seeds of polymers with the "matched" multiblock architecture. To provide further support for this unexpected result, we attempted to induce the growth of PFS_{26}-*b*-$PDMS_{584}$-*b*-PFS_{26} unimers from a pure sample of PFS_{26}-*b*-$PDMS_{292}$ seeds (L_n = 102 nm) and also to grow PFS_{26}-*b*-$PDMS_{292}$ unimers from PFS_{26}-*b*-$PDMS_{584}$-*b*-PFS_{26} seeds (L_n = 94 nm). Investigation of the contour lengths in TEM micrographs after 12 h (L_n = 114 nm and 107 nm, respectively, Figure S6), indicated that both sets of seed micelles failed to induce significant growth of added unimer possessing the mismatched multiblock architecture. Although a convincing explanation for this unexpected phenomenon requires more detailed studies it suggests that the nature of the corona in the seed and incoming unimer plays a key role in determining

whether epitaxial growth is efficient.

Summary

An A-B-A triblock copolymer with two crystallizable PFS terminal "A' blocks and a narrow molecular weight distribution was obtained by a two-step methodology. Fiber-like micelles with coronas in a looped configuration could be formed in the mixed solvent system of hexane and decane (*v*:*v*, 1:1). The formation of uniform cylindrical micelles was achieved by the use of a living CDSA seeded-growth approach. Low dispersity samples of fiber-like micelles with lengths controlled over the range of 100 nm to 2 μm were accessed through alterations of the seed-to-unimer ratio. We also performed studies on the living CDSA of the PFS_{26}-*b*-$PDMS_{584}$-*b*-PFS_{26}/PFS_{26} blends using PFS_{26}-*b*-$PDMS_{584}$-*b*-PFS_{26} cylindrical micelle seeds. This yielded ribbon-like micelles. Surprisingly, we found that the growth of PFS_{26}-*b*-$PDMS_{584}$-*b*-PFS_{26} and PFS_{26}-b-$PDMS_{292}$ were only successfully induced by seeds with the matched multiblock structure. This suggests that the corona on the seed and unimer plays a key role in determining whether growth via the living CDSA method is successful and further studies are underway to investigate this interesting phenomenon in more detail.

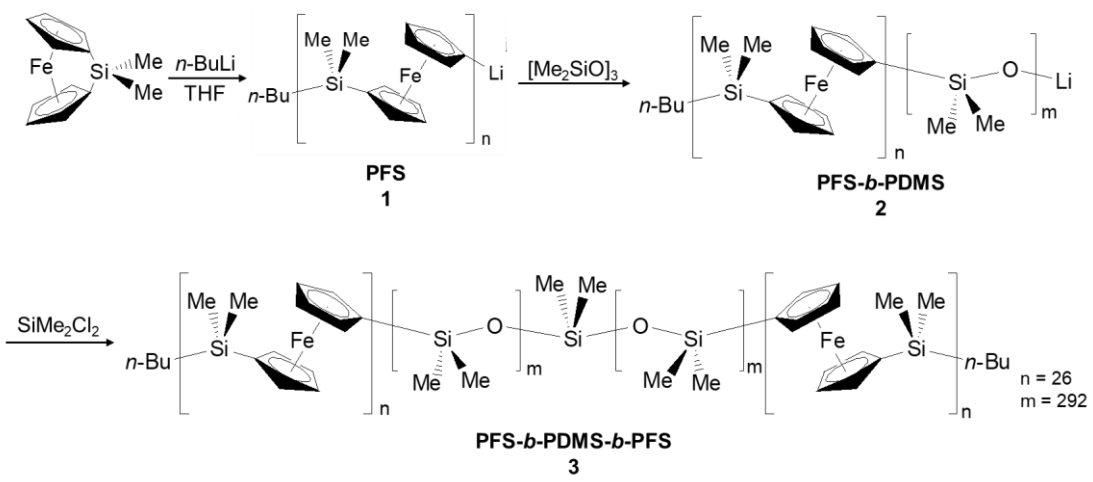

Figure 1. Synthesis of PFS_{26}-*b*-$PDMS_{584}$-*b*-PFS_{26} triblock copolymer.

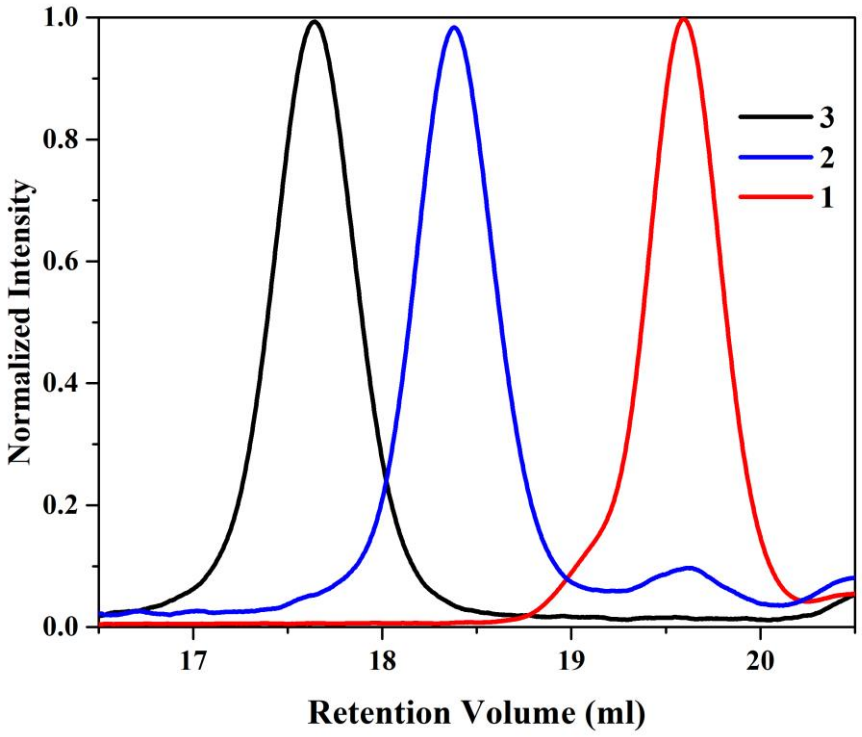

Figure 2. GPC chromatographs (refractive index response) in THF of purified triblock copolymer **3** (PFS_{26}-*b*-$PDMS_{584}$-*b*-PFS_{26}, PDI = 1.05), and its precursors **2** (PFS_{26}-*b*-$PDMS_{292}$, PDI = 1.07) and **1** (PFS_{26}, PDI = 1.04).

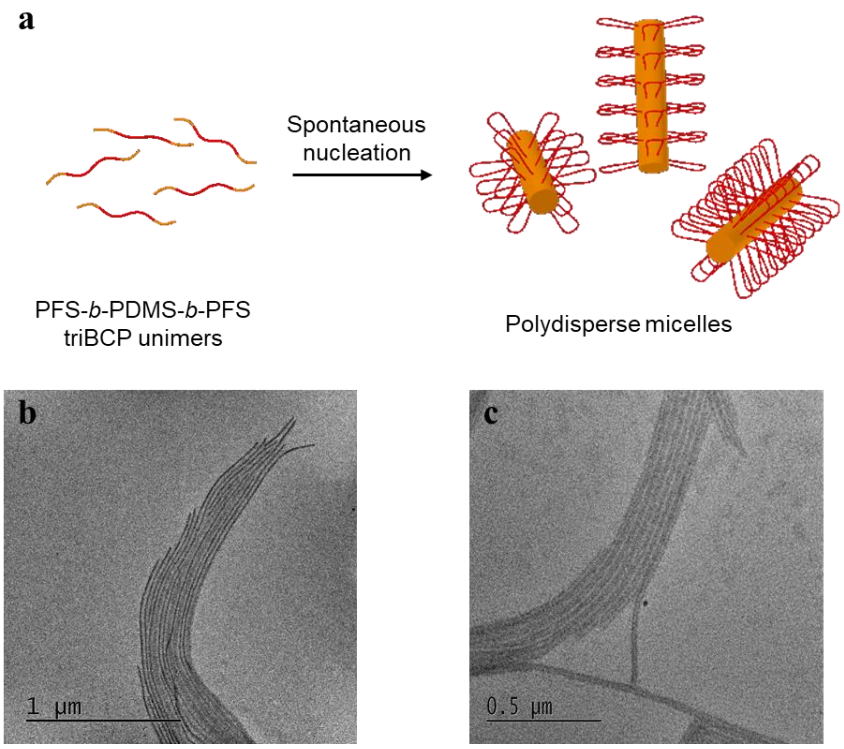

Figure 3. (a) A schematic representation of "flowerlike" cylindrical micelle formation assuming an adjacent re-entry model. (b) TEM micrograph of cylindrical micelles of PFS_{26}-*b*-$PDMS_{584}$-*b*-PFS_{26} prepared by self-nucleation in a mixed solvent system (hexane/decane, *v*:*v* = 1:1). (c) Higher magnification TEM micrograph of the individual micelles.

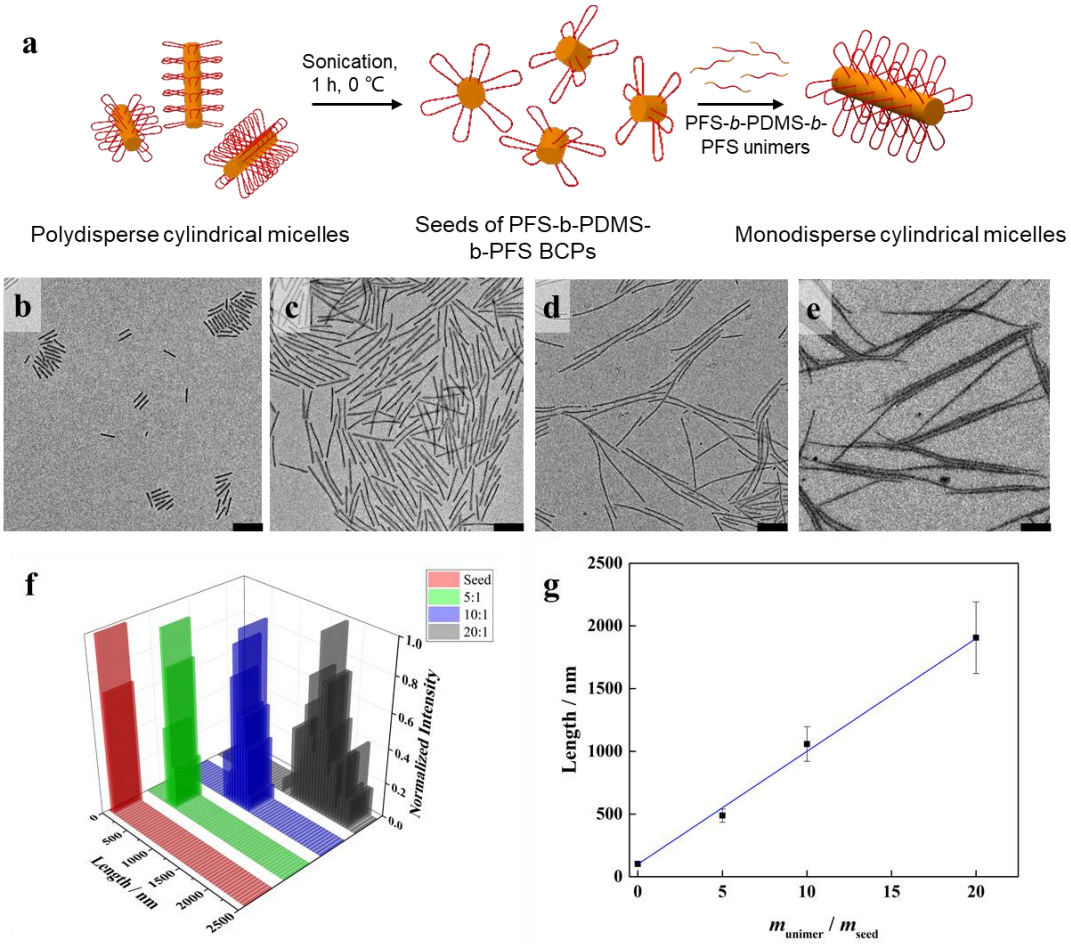

Figure 4. (a) A schematic representation of the preparation of monodisperse cylindrical micelles with looped corona from PFS_{26}-*b*-$PDMS_{584}$-*b*-PFS_{26} triblock copolymer assuming an adjacent re-entry model. TEM micrographs of near monodisperse cylindrical micelles (b) seed micelles of PFS_{26}-*b*-$PDMS_{584}$-*b*-PFS_{26} (L_n = 102 nm) (c) 5 equiv, (d) 10 equiv and (e) 20 equiv of PFS_{26}-*b*-$PDMS_{584}$-*b*-PFS_{26} unimer. Scale bars are 250 nm. (f) Histograms showing the contour length distribution of cylindrical micelles of PFS_{26}-*b*-$PDMS_{584}$-*b*-PFS_{26} prepared by living CDSA seeded growth methods. Legend in the top right denotes the unimer-to-seed ratio. (L_w/L_n = 1.02, 1.01, 1.02 and 1.02, respectively) (g) Graph showing the linear dependence of micelle length on the unimer-to-seed ratio of PFS_{26}-*b*-$PDMS_{584}$-*b*-PFS_{26}. The contour lengths measured from TEM images were slightly lower than the theoretical values based on the unimer to seed ratio. This may be a consequence of small amounts of remaining unimer or self-nucleation.

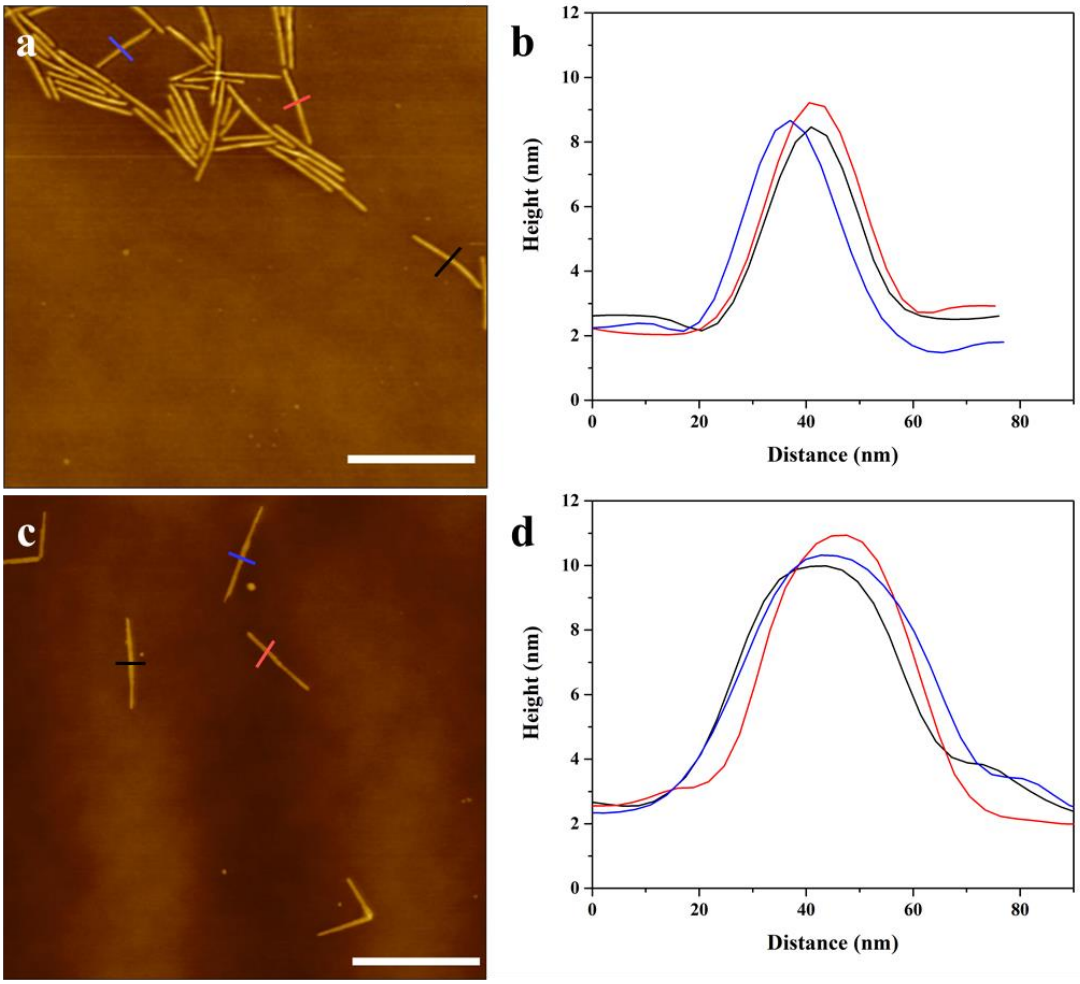

Figure 5. (a) AFM height image of PFS_{26}-*b*-$PDMS_{584}$-*b*-PFS_{26} seed micelles (L_n = 102 nm) on a carbon-coated TEM grid. (b) Height profiles across three single seed micelles of PFS_{26}-*b*-$PDMS_{584}$-*b*-PFS_{26}. (c) AFM height image of PFS_{26}-*b*-$PDMS_{292}$ seed micelles (L_n = 112 nm) on a carbon-coated TEM grid. (d) Height profiles across three single seed micelles of PFS_{26}-*b*-$PDMS_{292}$. The scale bar corresponds to 200 nm.

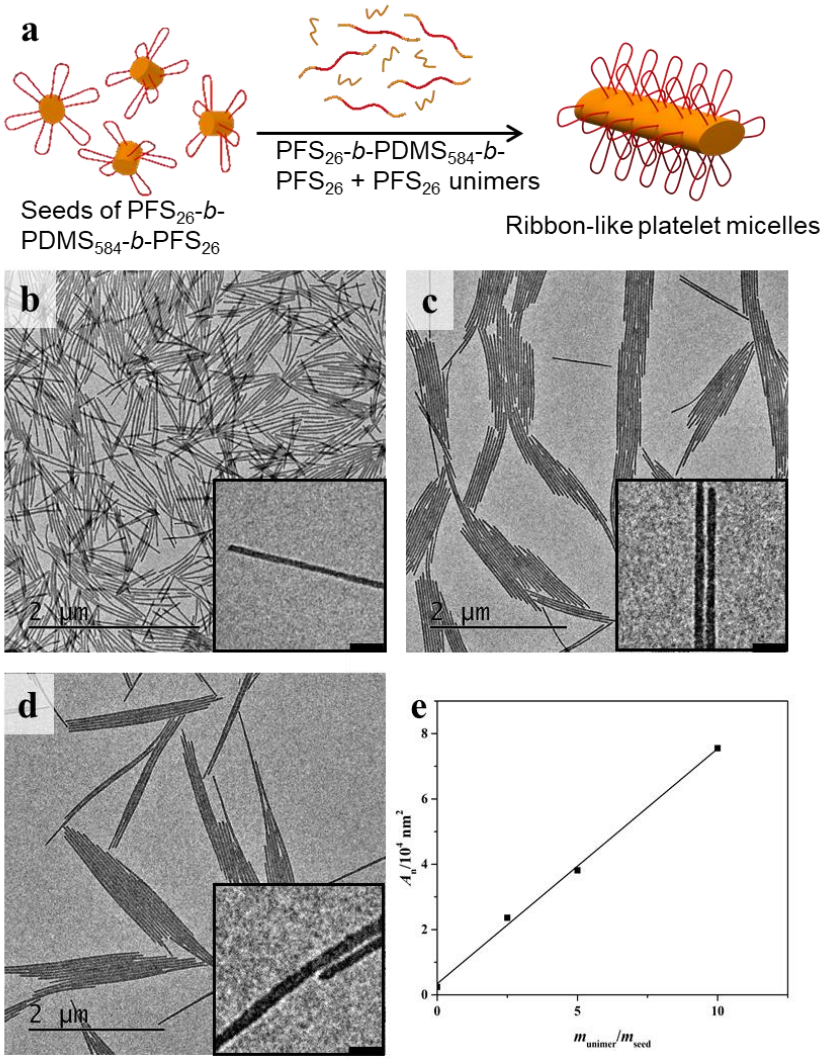

Figure 6. (a) Schematic diagram of living CDSA of the PFS_{26} / PFS_{26}-*b*-$PDMS_{584}$-*b*-PFS_{26} blend unimers in the PFS_{26}-*b*-$PDMS_{584}$-*b*-PFS_{26} cylindrical micelle seeds (L_n = 102 nm) in mixed solvent (hexane/decane, v : v = 1 : 1). (b-d) TEM micrographs of ribbon-like platelet micelles formed with unimer (total) to seed mass ratios of 2.5 : 1 (b), 5 : 1 (c) and 10 : 1 (d) at room temperature. (e) Linear dependence of micelle area on the unimer to seed mass ratio. Scale bars are (insets of b-d) 100 nm.

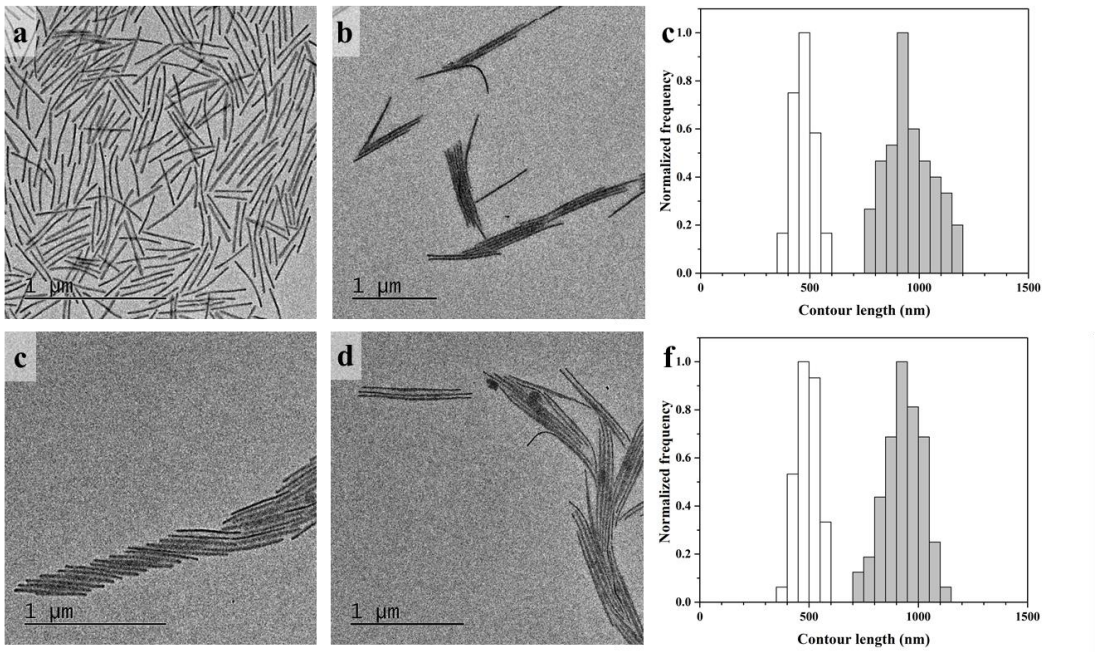

Figure 7. (a)-(c) TEM micrographs of cylindrical micelles obtained by adding (a) 10 and (b) 20 equivalents of PFS_{26}-*b*-$PDMS_{292}$/PFS_{26}-*b*-$PDMS_{584}$-*b*-PFS_{26} blend unimers to PFS_{26}-*b*-$PDMS_{584}$-*b*-PFS_{26} seed micelles (L_n = 102 nm); (c) histograms showing the contour length distribution of samples. (d)-(f) TEM micrographs of cylindrical micelles obtained by adding (d) 10 and (e) 20 equivalents of PFS_{26}-*b*-$PDMS_{292}$/PFS_{26}-*b*-$PDMS_{584}$-*b*-PFS_{26} blend unimers to PFS_{26}-*b*-$PDMS_{292}$ seed micelles (L_n = 112 nm); (f) histograms showing the contour length distribution of samples where the L_w/L_n values varied from 1.03 to 1.01.

References

1. Y. Mai and A. Eisenberg, *Chem. Soc. Rev.*, 2012, **41**, 5969-5985.
2. A. H. Gröschel and A. H. E. Müller, *Nanoscale*, 2015, **7**, 11841-11876.
3. F. H. Schacher, P. A. Rupar and I. Manners, *Angew. Chem. Int. Ed.*, 2012, **51**, 7898-7921.
4. U. Tritschler, S. Pearce, J. Gwyther, G. R. Whittell and I. Manners, *Macromolecules*, 2017, **50**, 3439-3463.
5. S. V. Vinogradov, T. K. Bronich and A. V. Kabanov, *Adv. Drug Delivery Rev.*, 2002, **54**, 135-147.
6. Z. Ge and S. Liu, *Chem. Soc. Rev.*, 2013, **42**, 7289-7325.
7. J. Schöbel, M. Burgard, C. Hils, R. Dersch, M. Dulle, K. Volk, M. Karg, A. Greiner and H. Schmalz, *Angew. Chem. Int. Ed.*, 2017, **56**, 405-408.
8. H.-C. Kim, S.-M. Park and W. D. Hinsberg, *Chem. Rev.*, 2010, **110**, 146-177.
9. S.-J. Park, S.-G. Kang, M. Fryd, J. G. Saven and S.-J. Park, *J. Am. Chem. Soc.*, 2010, **132**, 9931-9933.
10. A. O. Moughton, M. A. Hillmyer and T. P. Lodge, *Macromolecules*, 2012, **45**, 2-19.
11. C. Chassenieux, T. Nicolai and L. Benyahia, *Curr. Opin. Colloid Interface Sci.*, 2011, **16**, 18-26.
12. T. Zinn, L. Willner and R. Lund, *ACS Macro Lett.*, 2016, **5**, 1353-1356.
13. C. Gourier, E. Beaudoin, M. Duval, D. Sarazin, S. Maître and J. François, *J. Colloid Interface Sci.*, 2000, **230**, 41-52.
14. Z. Xie, T. Lu, X. Chen, C. Lu, Y. Zheng and X. Jing, *J. Appl. Polym. Sci.*, 2007, **105**, 2271-2279.
15. A. J. de Graaf, K. W. M. Boere, J. Kemmink, R. G. Fokkink, C. F. van Nostrum, D. T. S. Rijkers, J. van der Gucht, H. Wienk, M. Baldus, E. Mastrobattista, T. Vermonden and W. E. Hennink, *Langmuir*, 2011, **27**, 9843-9848.
16. J. Jin, D. Wu, P. Sun, L. Liu and H. Zhao, *Macromolecules*, 2011, **44**, 2016-2024.
17. J. E. Nielsen, K. Zhu, S. A. Sande, L. Kováčik, D. Cmarko, K. D. Knudsen and B. Nyström, *J. Phys. Chem. B*, 2017, **121**, 4885-4899.
18. S. Honda, T. Yamamoto and Y. Tezuka, *J. Am. Chem. Soc.*, 2010, **132**, 10251-10253.
19. V. S. Kadam, E. Nicol and C. Gaillard, *Macromolecules*, 2012, **45**, 410-419.
20. T. Zinn, L. Willner, K. D. Knudsen and R. Lund, *Macromolecules*, 2017, **50**, 7321-7332.
21. X. Zhao, W. Liu, D. Chen, X. Lin and W. W. Lu, *Macromol. Chem. Phys.*, 2007, **208**, 1773-1781.
22. S. Li, Y. Su, M. Dan and W. Zhang, *Polym. Chem.*, 2014, **5**, 1219-1228.
23. W. Wang, C. Gao, Y. Qu, Z. Song and W. Zhang, *Macromolecules*, 2016, **49**, 2772-2781.
24. J. Schöbel, M. Karg, D. Rosenbach, G. Krauss, A. Greiner and H. Schmalz, *Macromolecules*, 2016, **49**, 2761-2771.
25. J. C. Foster, S. Varlas, B. Couturaud, Z. Coe and R. K. O'Reilly, *J. Am. Chem. Soc.*, 2019, **141**, 2742-2753.
26. X. Wang, G. Guerin, H. Wang, Y. Wang, I. Manners and M. A. Winnik, *Science*, 2007, **317**, 644-647.
27. H. Qiu, Y. Gao, C. E. Boott, O. E. C. Gould, R. L. Harniman, M. J. Miles, S. E. D. Webb, M. A. Winnik and I. Manners, *Science*, 2016, **352**, 697-701.
28. R. L. N. Hailes, A. M. Oliver, J. Gwyther, G. R. Whittell and I. Manners, *Chem. Soc. Rev.*, 2016, **45**, 5358-5407.
29. N. Petzetakis, A. P. Dove and R. K. O'Reilly, *Chem. Sci.*, 2011, **2**, 955-960.
30. D. Tao, C. Feng, Y. Cui, X. Yang, I. Manners, M. A. Winnik and X. Huang, *J. Am. Chem. Soc.*,

2017, **139**, 7136-7139.
31. I. Choi, S. Yang and T.-L. Choi, *J. Am. Chem. Soc.*, 2018, **140**, 17218-17225.
32. X.-H. Jin, M. B. Price, J. R. Finnegan, C. E. Boott, J. M. Richter, A. Rao, S. M. Menke, R. H. Friend, G. R. Whittell and I. Manners, *Science*, 2018, **360**, 897-900.
33. J. Qian, X. Li, D. J. Lunn, J. Gwyther, Z. M. Hudson, E. Kynaston, P. A. Rupar, M. A. Winnik and I. Manners, *J. Am. Chem. Soc.*, 2014, **136**, 4121-4124.
34. J. Schmelz, M. Karg, T. Hellweg and H. Schmalz, *ACS Nano*, 2011, **5**, 9523-9534.
35. J. Schmelz, A. E. Schedl, C. Steinlein, I. Manners and H. Schmalz, *J. Am. Chem. Soc.*, 2012, **134**, 14217-14225.
36. A. M. Oliver, J. Gwyther, M. A. Winnik and I. Manners, *Macromolecules*, 2018, **51**, 222-231.
37. R. Resendes, J. A. Massey, K. Temple, L. Cao, K. N. Power-Billard, M. A. Winnik and I. Manners, *Chem. - Eur. J.*, 2001, **7**, 2414-2424.
38. K. Temple, F. Jäkle, J. B. Sheridan and I. Manners, *J. Am. Chem. Soc.*, 2001, **123**, 1355-1364.
39. Y. Ni, R. Rulkens and I. Manners, *J. Am. Chem. Soc.*, 1996, **118**, 4102-4114.
40. R. A. Musgrave, A. D. Russell and I. Manners, *Organometallics*, 2013, **32**, 5654-5667.
41. J. B. Gilroy, T. Gädt, G. R. Whittell, L. Chabanne, J. M. Mitchels, R. M. Richardson, M. A. Winnik and I. Manners, *Nat. Chem.*, 2010, **2**, 566-570.

Acknowledgements

Q.Z. is grateful to the Chinese Scholarship Council (CSC) for a visiting studentship. J.L. and Y.L. thank the financial support from National Natural Science Foundation of China (Grant No. 11632005, 11672086). We also thank L. MacFarlane and X. Jin for helpful discussions and suggestions.